MOLECULAR TECHNIQUES AND MODEL SYSTEMS IN THE STUDY OF INFECTIOUS DISEASES

A Thesis Presented for the

Master of Science

Degree

The University of Tennessee, Knoxville

Jemma McLeish

December 2025

Copyright © 2025 by Jemma McLeish

All rights reserved.

ABSTRACT

The demand for novel models and molecular techniques to better understand microbial pathogenesis has been motivated by the rising incidence of bacterial and fungal infections worldwide as well as the development of antibiotic and antifungal drug resistance. This study investigated the function of virulence-related genes and host-pathogen interactions using *Candida glabrata*, *Candida albicans*, and entomopathogenic *Xenorhabdus* species. The study sought to analyze the functions of *STE11* and *CHO1*, examine virulence in *Manduca sexta* larvae, and evaluate MAPK signalling using molecular genetic approaches, functional complementation, western blotting, and non-mammalian infection models.

A truncation mutant of *C. glabrata STE11 (STE11$^{\Delta N346}$)* was successfully constructed and expressed via an episomal vector, pGRB2.1. Western blot analysis indicated that the truncation did not alter MAPK activation, suggesting a divergence from *C. albicans* regulatory pathways. Functional complementation in *Saccharomyces cerevisiae cho1Δ* mutants confirmed that *CgCHO1* encodes a phosphatidylserine (PS) synthase, highlighting its conserved role in lipid biosynthesis and stress adaptation.

The *M. sexta* infection model successfully recapitulated virulence phenotypes observed in murine models, including the reduced virulence of *C. albicans STE11ΔN467* mutants. The model was subsequently applied to assess the entomotoxic potential of *Xenorhabdus* species, revealing strain-specific differences in virulence and supporting the broader utility of this model in studying host-pathogen interactions across microbial kingdoms.

TABLE OF CONTENTS

LIST OF TABLES

LIST OF FIGURES

CHAPTER ONE

INTRODUCTION AND LITERATURE REVIEW

Significance

Fungal and bacterial infections remain a major global health burden, especially for hospitalized and immunocompromised populations. Among the primary causes of invasive candidiasis, a disease in which *Candida* species invade the surface and spread into sterile areas like the blood and deep organs with a high mortality rate, are opportunistic species such as *Candida albicans* and *Nakaseomyces glabrata* (formerly called *Candida glabrata*, which will be used throughout this document) (Beardsley et al., 2024; Brown et al., 2012; Pappas, Lionakis, Arendrup, Ostrosky-Zeichner, & Kullberg, 2018; Ricotta et al., 2021). Furthermore, although mainly studied in insect models, the Gram-negative bacteria *Xenorhabdus* species provide valuable insights into bacterial pathogenicity and their role in the relationships among organisms within entomopathogenic cycles. These organisms can be regarded as models of infections, with specific examples provided in this study (Goodrich-Blair & Clarke, 2007).

Candida species are ubiquitous fungi that are part of the human microbiome, but under certain conditions, such as immunocompromised states seen in HIV/AIDS-positive populations, use of immunosuppressants during chemotherapy and solid-organ transplants, chronic illness, old age, and nosocomial infections, especially in newborns, these organisms can spread and cause a range of infections, from superficial to invasive (Brown et al., 2012; Cottier & Hall, 2020). A major clinical concern is the increasing prevalence of fungal infections, particularly given the growing resistance to widely used

antifungal drugs such as azoles and echinocandins (Kondaka et al., 2025). *C. albicans* remains one of the most frequently isolated fungal pathogens in clinical settings, and its virulence characteristics have been well-documented, including morphological plasticity (yeast to hyphal switching), adhesion to host tissues, biofilm formation, and an ability to evade host responses (Mayer, Wilson, & Hube, 2013). *C. glabrata* is another common *Candida* species that also causes severe infections, but its documented virulence traits differ from those of *C. albicans*, such as its ability to persist within host macrophages and its lack of filamentous morphology (Brunke & Hube, 2013; Healey & Perlin, 2018). Both of these species have shown increased resistance to frontline antifungal drugs like azoles, echinocandins, and polyenes (Bhattacharya, Sae-Tia, & Fries, 2020).

In addition to fungal pathogens, both Gram-negative and Gram-positive bacteria have been linked to 750,000 fatalities worldwide, including *Staphylococcus aureus*, *Escherichia coli*, *Streptococcus pneumoniae*, and *Klebsiella pneumoniae* (Ikuta et al., 2022).

For this study, Gram-negative bacteria of the *Xenorhabdus* species are used to provide valuable insights into bacterial virulence and enhance the value of an insect model for infection (Goodrich-Blair & Clarke, 2007). Members of the genus *Xenorhabdus*, which are entomopathogenic nematode symbionts, are known for their diverse range of virulence factors, including released toxins and antimicrobial peptides, and for their potent insecticidal properties (McQuade & Stock, 2018). During an infection, these bacteria are spontaneously introduced into insect hosts and retain a mutualistic relationship with *Steinernema* nematodes. A variety of virulence factors, such

as toxins and immunomodulatory substances, are secreted by *Xenorhabdus* species upon entering the hemolymph, aiding host colonization and nematode development (Goodrich-Blair & Clarke, 2007). Even though these bacteria are not commonly associated with human infections, they are useful comparative models for studying host-pathogen interactions because they can modify the host immune response and produce bioactive molecules.

The rising occurrence of antimicrobial resistance in bacterial and fungal infections is a significant concern. Especially troubling are C. glabrata and the emerging C. auris, which have shown increasing resistance to frontline antifungal medications (Hetzler, Kollef, Yuenger, Micek, & Betthauser, 2022; Hickson, Ledger, & Wells, 2025; Pfaller, Diekema, Turnidge, Castanheira, & Jones, 2019).

The development of targeted therapeutics relies on our expanding knowledge of the mechanisms behind drug resistance and microbial pathogenesis. In laboratory settings, researchers can analyze gene function, describe virulence pathways, and evaluate potential therapeutic interventions by combining genetic techniques with in vivo infection models, such as the *Manduca sexta* caterpillars.

Traditional models of systemic infections, such as vertebrates

Numerous animal hosts have been used in scientific research for their distinct biological and physiological characteristics, making them suitable models for studying human diseases. The selection of an appropriate infection model depends on several factors, including host susceptibility to the illness, animal size, cost, housing requirements, reagent availability, risk of coinfection, and ethical constraints. Some of

these model organisms include mice, rats, guinea pigs, hamsters, rabbits, ferrets, chickens, zebrafish, insects, and non-human primates (Trevijano-Contador & Zaragoza, 2014; Tsai, Loh, & Proft, 2016).

Mice and rats are widely used for their reproducibility and availability of extensive immunological and genetic tools (Sarkar & Heise, 2019). Ferrets are often used to study respiratory pathogens such as influenza and SARS-CoV-2 because their lung physiology closely resembles that of humans (Oh & Hurt, 2016; Zhao et al., 2023). Insect models such as *Galleria mellonella* and *M. sexta* are used for their rapid growth, small size, and short life cycle, which are some of the ideal qualities that a good *in vivo* model must have to be beneficial (Giammarino, Bellucci, & Angiolella, 2024; Lyons et al., 2020). Non-human primates, including rhesus macaques, are selected for investigations in which the pathogenesis and immune responses must closely approximate those observed in human infections (Gardner & Luciw, 2008).

Among these, murine models remain the most widely used for studying host-pathogen interactions, including candidiasis. This model has provided essential insights into identifying fungal virulence factors, immune evasion strategies, host immune pathways, and evaluating antifungal therapeutic efficacy due to their similarity to humans (Pappas et al., 2018). Furthermore, studies in mice have been instrumental in elucidating immune signaling pathways such as Toll-like receptor activation and neutrophil recruitment in response to fungal infection (Lionakis & Netea, 2013).

Despite their advantages, the use of vertebrate models is constrained by ethical considerations, high maintenance costs, and regulatory oversight, which makes them less

suitable for high-throughput screening. These disadvantages have contributed to the growing interest in alternative invertebrate models that enable rapid, inexpensive evaluation of host-pathogen interactions.

Manduca sexta as a non-mammalian host

Insects are among the most widely used animals in research. For example, Garcia-Bustos et al. used *Galleria mellonella* as an *in vivo* model to assess interactions between the insect and *Candida* species (Garcia-Bustos et al., 2022). Also, Lyons et al. conducted a study that established *M. sexta* as an *in vivo* model for measuring fungal virulence of *C. albicans* and *C. glabrata* and for assessing drug efficacy (Lyons et al., 2020).

Invertebrate models have become advantageous alternatives for conventional vertebrate systems for examining host-pathogen interactions. Their advantages include low maintenance costs, high experimental throughput, reduced ethical constraints, and a robust innate immune system comparable to that of mammals. For instance, *M. sexta* larvae possess conserved immune system pathways, such as Toll, immune deficiency (IMD), and Jun N-terminal kinase (JNK) signaling, as well as effector mechanisms like melanization, phagocytosis, and antimicrobial peptide production (Eleftherianos, Clarke, Dowling, & Reynolds, 2010; Lyons et al., 2020).

The fifth instar larval stage is commonly used for systemic infection models. Pathogens, including *Candida* or *Xenorhabdus* species, can be injected directly into the hemocoel between the first abdominal prolegs, which facilitates consistent delivery of pathogen doses (Hussa & Goodrich-Blair, 2012; Lyons et al., 2020).

Recent studies have shown that *M. sexta* can recapitulate known virulence phenotypes observed in mammalian models. For instance, *C. albicans STE11*$^{\Delta N467}$ mutants, previously shown to exhibit attenuated virulence in murine models, demonstrated a similarly reduced ability to kill *M. sexta* larvae (T. Chen, Jackson, et al., 2019; McLeish, 2021b). These results support the use of *M. sexta* for identifying genes and pathways involved in fungal pathogenicity.

Although *M. sexta* has demonstrated effectiveness as a model for fungal pathogenesis, its application has expanded to include bacterial pathogens, particularly those associated with insects such as *Xenorhabdus*. These Gram-negative bacteria exist in a mutualistic relationship with entomopathogenic nematodes of the genus *Steinernema* and play a critical role in killing the insect host during the parasitic stage of their life cycle. Once inside the insect's hemocoel, *Xenorhabdus* species secrete a wide range of metabolites that disrupt host immunity, degrade tissues, and destroy competing microbes, which ultimately promotes nematode reproduction (Goodrich-Blair & Clarke, 2007; Hussa & Goodrich-Blair, 2012).

M. sexta serves as an ideal host for assessing the virulence properties of different *Xenorhabdus* strains. Bacterial cultures of these strains can be injected into fifth-instar larvae to provide accurate dose control and repeatable results. The ability to model both fungal and bacterial infections within the same host context enhances the versatility of the *M. sexta* system. It enables researchers to explore conserved innate immune responses, such as melanization and antimicrobial peptide expression, across taxonomically distinct pathogens. Additionally, this model supports broader questions in

infection biology, such as microbial competition, polymicrobial infections, and host specificity.

Research rationale

Despite many studies on the biology of *Candida* species, there remain critical gaps in our understanding of species-specific virulence mechanisms of *C. albicans* and the general biology of *C. glabrata*. Also, the functions of non-fungal pathogens, such as *Xenorhabdus* species, in model infection systems are still poorly understood, especially regarding host immune regulation and comparisons of pathogenesis between species. In this study, I present two general approaches to investigate host-pathogen interactions: (1) using genetic manipulations to study gene functions and signaling in *Candida* species and (2) using the insect host *Manduca sexta* to compare virulence phenotypes within *Xenorhabdus* and *Candida* strains. The combination of methods, including western blotting, colony PCR, yeast and bacterial transformation, and Gibson assembly, provides a comprehensive analysis of gene expression and pathway function. The overarching objective of this research project is to validate *M. sexta* as a highly efficient model for systemic infection and to identify functional gene targets to inform antifungal drug discovery and treatment design.

Parts of this research has been published by Heppert, J. K., Awori, R. M., Cao, M., Chen, G., McLeish, J., & Goodrich-Blair, H. (2024a). Analyses of *Xenorhabdus griffiniae* genomes reveal two distinct sub-species that display intra-species variation due to prophages.

CHAPTER TWO

MATERIALS AND METHODS

Experimental overview

This present study investigated host-pathogen interactions using a molecular biology approach, focusing on *Candida glabrata*, *Candida albicans,* and *Xenorhabdus* species as microbial pathogens. *Manduca sexta* fifth instar larvae served as a non-mammalian *in vivo* infection model to assess pathogenicity. The overarching goal was to apply experimental methodologies for the functional characterization of target genes and assessment of virulence traits, with a broader aim of contributing to antifungal drug discovery efforts. A multidisciplinary approach was employed, incorporating molecular biology, microbiology, and *in vivo* experimental techniques. These included polymerase chain reaction (PCR), molecular cloning, *Escherichia coli* and yeast transformation, Gibson assembly, western blotting, and survival assays in *M. sexta* larvae.

Strains and plasmids growth conditions

The strains and plasmids utilized in this study are listed in Tables 2.1 and 2.2, respectively. *C. glabrata*, *C. albicans,* and *S. cerevisiae* strains were routinely cultured in yeast extract peptone dextrose (YPD) medium (% w/vol, 1% yeast extract, 2% peptone, and 2% dextrose) with shaking incubation at approximately 200 rpm. For the selection of yeast transformants, synthetic complete (SC) medium (% w/vol, 2% dextrose, 0.67% yeast nitrogen base without amino acids, and 0.79g/L Complete Supplement Mixture without Histidine and Uracil (CSM-HIS-URA) double dropout supplement). Where applicable, nourseothricin was added at a final concentration of 100 μg/mL for the

selection of strains harboring the NAT1 resistance marker, and 1 mM ethanolamine for cho1Δ mutant growth. Yeast cell culture density was monitored by measuring optical density at 600 nm (OD_{600}) using a spectrophotometer.

E. coli DH5α (New England Biolabs) was employed for plasmid propagation and was grown in Luria–Bertani (LB) media (tryptone 10g/L, yeast extract 5g/L, and sodium chloride 10 g/L) at 37 °C supplemented with 100 µg/mL ampicillin. Plasmid DNA was extracted using QIA prep Spin Miniprep Kit (Qiagen) following the manufacturer's protocol. The constructs were then validated via restriction enzyme digestion, PCR, and Sanger sequencing. All strains and plasmids were preserved in 25 % (v/v) glycerol stocks at -80 °C for long-term storage.

Strains and plasmids construction

The primers used in this study are described in Table 2.3. Plasmid design and assembly of plasmids were conducted using standard molecular cloning techniques (Bertero, Brown, & Vallier, 2017; Green & Sambrook, 2012; Kaiser, Michaelis, & Mitchell, 1994). Polymerase Chain Reaction (PCR) amplification was performed using high-fidelity DNA polymerase (New England Biolabs) according to the manufacturer's instructions.

DNA fragments used for cloning were amplified from either genomic DNA or existing plasmid templates, employing primers containing restriction enzyme sites or homology arms as required for downstream assembly.

Construction of *C. glabrata* STE11$^{\Delta N346}$ truncation mutant

An initial attempt to generate the *C. glabrata STE11$^{\Delta N346}$* truncation mutant was done using the pRS316 shuttle vector, often used for *Saccharomyces cerevisiae* cloning (Sikorski & Hieter, 1989). The truncated *STE11$^{\Delta N346}$* allele was PCR-amplified from genomic DNA and cloned into the pRS316 vector using restriction cloning with KpnI and BamHI restriction sites, followed by transformation into the wild-type strain Cg1. Based on the obtained transformants, the verification procedures by colony PCR and restriction digestions showed that obtaining the mutant strain via this method was unsuccessful and unlikely. Furthermore, despite repeated attempts at plasmid reconstructions, numerous troubleshooting strategies, and tedious transformation attempts, this plasmid was determined to be unsuitable for use in *C. glabrata* for this purpose due to compatibility issues identified. The compatible issue identified was the absence of a *C. glabrata* species-specific CEN/ARS region.

Consequently, a new construct was generated by cloning the PCR-amplified *STE11$^{\Delta N346}$* insert into the episomal plasmid pGRB2.1 (p157), a shuttle vector used in *C. glabrata* expression cloning (Zordan et al., 2013). This was achieved using the same molecular cloning strategy as stated before, facilitating expression of the *STE11$^{\Delta N346}$* truncated allele and enabling downstream phenotypic analyses. The recombinant plasmid construct was confirmed by restriction digestion, colony PCR, and Sanger sequencing before transformation into the wild-type strain, Cg1.

Construction of *C. albicans* $STE11^{\Delta N467}$ in clinical isolates

Generation of the $STE11^{\Delta N467}$ *C. albicans* mutant strains in clinical isolates was attempted by PCR-amplifying the truncated $STE11^{\Delta N467}$ allele from the previously constructed DAY286 $STE11^{\Delta N467}$ mutant strain. The DAY286 strain was used as the background for generating the $STE11^{\Delta N467}$ mutant, as it is one of the strains commonly used in laboratory settings and is derived from the BWP17 parent strain (Richard, Nobile, Bruno, & Mitchell, 2005). The BWP17 strain is a derivative of the commonly used laboratory strain, SC5314 (Selmecki, Bergmann, & Berman, 2005). Briefly, the truncation allele was PCR-amplified from genomic DNA using primers flanking the deleted region. The resulting DNA fragment was purified and then transformed into the clinical isolates p87, p75010, p57055, and p76067 via electroporation. This selection of strains was purposefully chosen as they represent intraspecies variation, with isolates from diverse infection sites, distinct genetic clades, and exhibit varying phenotypic characteristics (Huang, Woolford, May, Mcmanus, & Mitchell, 2019). For example, p87 (clade 4) was isolated from an oral infection, while p75010 (clade 11), p57055 (clade 3), and p76067 (clade 2) were isolated from bloodstream infections (Xiong, Goerlich, Do, & Mitchell, 2024). Despite multiple transformation attempts, stable integration of the truncation allele was not achieved using this approach.

Construction of *C. glabrata* Cho1Δ mutant

C. glabrata wild-type strain Cg1 was the parental background for the generation of the CgCho1Δ mutant. Approximately 500 bp of the upstream and downstream flanking regions of the *CgCHO1* locus were PCR-amplified from Cg1 genomic DNA. These

flanking sequences were cloned into the integrating shuttle vector pRS306 using HindIII and EcoRI restriction sites, resulting in the plasmid pCgCho1Δ. This plasmid was then transformed into Cg1 via electroporation following the lithium acetate method described for *S. cerevisiae* (Gietz & Schiestl, 2007).

In addition to generating a markerless deletion mutant, a second mutant was constructed by replacing the *CgCHO1* open reading frame (ORF) with a Nourseothricin resistance cassette (NAT1). To do this, the NAT1 fragment was introduced into the HindIII and EcoRI restriction sites of pCgCho1Δ to generate the plasmid, pCgCho1Δ+NAT1. All constructs were verified by PCR screening, restriction enzyme digestion, and Sanger sequencing.

Construction of a conditional *CgCHO1* expression strain

To generate a CgCho1Δ that conditionally expressed *CgCHO1* under the regulation of the TET promoter, the plasmid pCgCho1Δtet was constructed. DNA fragments were generated by PCR amplifying *CgCHO1* using high-fidelity DNA polymerase (New England Biolabs) with primers designed to amplify the 5' untranslated region (UTR) and approximately 500 bp of *CgCHO1* ORF. These PCR products, along with the vectors p97CGH, p99CGH, and pINTG4 were purified using the QIA quick Gel Extraction Kit (Qiagen) and quantified by spectrophotometry and assembled using Gibson Assembly (Nakayama et al., 1998). Briefly, equimolar amounts of vector and insert DNA were incubated at 50 °C for 60 minutes. The resulting assembled plasmids were transformed into chemically competent *E. coli* DH5α cells by heat shock and

selected on LB agar plates containing 100 µg/mL ampicillin. Positive clones were verified by colony PCR, restriction digestion, and Sanger sequencing.

Yeast transformation

Transformation of *C. glabrata* and *S. cerevisiae* was performed using a modified high-efficiency lithium acetate/single-stranded carrier DNA/polyethylene glycol (LiAc/SS-DNA/PEG) method, as previously described by Gietz and Schiestl (Gietz & Schiestl, 2007). Briefly, yeast cells were grown overnight in 5 mL of YPD medium in a shaking incubator set at 200 rpm at 30 °C. The next day, 100 µL of log phase cells were collected, washed once in 900 µL of ddH_2O, and measured using a hemocytometer to obtain $1x10^8$ cells mL^{-1}, which was then used for each transformation. These cells were then mixed with 240 µL of 50 % PEG 3350, 36 µL of 1.0 M lithium acetate, 50 µL of denatured salmon sperm DNA (2 mg/mL), and 34 µL of plasmid DNA and sterile water. The mixture was vortexed and heat-shocked at 42 °C for 40 minutes. Transformed cells were recovered in YPD medium at 30 °C for 2–3 hours and plated onto the appropriate selection media.

Transformation of clinical isolates of *C. albicans* (p87, p75010, p57055, and p76067) with the PCR-amplified truncated $STE11^{\Delta N467}$ allele from the previously constructed DAY286 S$TE11^{\Delta N467}$ mutant strain was carried out via electroporation by adopting a method previously described by De Backer *et. al.* (De Backer et al., 1999).To begin this process, overnight cultures were grown in YPD at 30 °C with shaking at 225 rpm to an OD_{600} of 1.6 - 2.2. Cells were harvested by centrifugation at 3,300 g for 5 minutes, and washed once with sterile water, followed by resuspension in Tris-EDTA

buffer and incubation with 1 M lithium acetate at 30 °C for 1 hour. Cells were then treated with 250 µL of 1 M DTT for 30 minutes, washed twice with ice-cold water, and once with 1 M sorbitol using centrifugation. Finally, cells were resuspended in 1 M sorbitol and used as electrocompetent cells.

For electroporation, 40 µL of competent cells were mixed with 5 µL of gel-purified DNA in a 0.2 cm electroporation cuvette. Electroporation was conducted at 1.8 kV, after which 1 mL of ice-cold 1 M sorbitol was added immediately. Cells were transferred to sterile tubes and plated on YPD agar supplemented with 200 µg/mL nourseothricin. Plates were incubated at 30 °C for 24- 48 hours. Transformants were selected based on nourseothricin resistance and later screened by PCR to confirm integration of the truncation allele.

Western blotting

C. glabrata and *C. albicans* cells were grown overnight in 5 mL YPD medium at 30 °C with agitation. The following day, cultures were reinoculated into 25 mL of fresh YPD at a starting OD_{600} of 0.1. The cultures were further incubated to mid-log phase to an OD_{600} of approximately 0.8, harvested by centrifugation, and washed with sterile distilled water. Cell pellets were transferred to orange screw-cap tubes, centrifuged again, and snap-frozen in liquid ethanol and dry ice or stored at −80 °C before protein extraction.

For protein isolation, frozen pellets were thawed on ice and resuspended in phosphate-buffered saline (PBS) supplemented with protease and phosphatase inhibitors (Roche). Cell lysis was performed in a cold room using glass bead disruption in a Bead

Beater with six cycles of one-minute agitation with one-minute rests on ice. Lysates were clarified by two rounds of centrifugation at 4 °C, first at 5,000 rpm for one minute, then for eight minutes, and the resulting supernatants were retained for protein purification. Protein concentration was determined using the Bradford assay with bovine serum albumin (BSA) standards, and absorbance was measured at 595 nm using a spectrophotometer (Bradford, 1976).

For SDS-PAGE, the protein samples were mixed with Laemmli loading buffer to a final protein concentration of 1 ng/µL and denatured by boiling at 90 °C for five minutes. Equal volumes of each sample (20 µL) were loaded onto 10% pre-cast polyacrylamide gels alongside a molecular weight ladder. Electrophoresis was performed at a constant voltage of 300 volts (V) and a current of 25-30 milliamperes (mA) for approximately two hours, or until the dye front reached the bottom of the gel.

Proteins were transferred onto nitrocellulose membranes using a wet transfer method at 400 mA for one hour at 4 °C. Membranes were then blocked for one hour at room temperature in a 1:1 mixture of Odyssey® Blocking Buffer (LI-COR Biosciences) and 1x Tris-buffered saline (TBS), then incubated with primary antibodies diluted in TBS with 0.1 % Tween-20 (TBST) supplemented with blocking buffer. Primary antibodies included rat anti-tubulin (5 µL) and rabbit anti-phospho-p44/42 MAPK polyclonal (5 µL, Cell Signaling Technology). After three washings, membranes were incubated with fluorescent secondary antibodies: goat anti-rat (1 µL) for tubulin and goat anti-rabbit (1 µL) for p44/42 MAPK. Membranes were washed and imaged using the Odyssey®

infrared imaging system (LI-COR Biosciences). Coomassie Blue staining was performed following transfer to verify equal protein loading across sample lanes.

Manduca sexta survival assay

Eggs of *Manduca sexta* (tobacco hornworm) were obtained from Carolina Biological Supply (North Carolina, USA) and were reared to the fifth instar according to a previously described protocol (Hussa & Goodrich-Blair, 2012). Briefly, eggs were sterilized with 0.6 % (v/v) bleach solution on arrival and then transferred to a four-ounce plastic container with a Gypsy moth diet (MP Biomedicals, Ohio, USA). The eggs were then incubated at 26 °C in a humidified insect incubator with a 16-h light: 8-h dark photoperiod. Once hatching was complete, the larvae were transferred to a new four-ounce container for two days and then transferred individually to a new two-ounce container. Feeding and cleaning were performed every two to three days until the larvae reached the fifth instar stage.

On the day of the assay, fifth instar larvae were examined and sorted by weight, ranging from 0.67 g to 3.5 g, and the larvae were randomly distributed across the conditions. Larvae (n =10 experimental group, with n = 5 for phosphate-buffered saline (PBS) control group) were placed into individual two-ounce plastic containers. Groups of 10 larvae were carefully injected with 10 µL of various doses (10^{-5}, 10^{-4}, and 10^{-3}) between the first set of abdominal prolegs using a 30-gauge Hamilton syringe. The following microbial bacterial and yeast strains used for infection were: *X. nematophila* (ATCC 19061), *X. innexi* (HGB1681), *X. griffiniae* (HGB2511 and ID10), and *Xenorhabdus* sp. TH1, *C. albicans* DAY286 wild-type and $STE11^{\Delta N467}$ mutant.

Following injection, the larvae were incubated at 26 °C in a humidified insect incubator with a 16-h light: 8-h dark photoperiod and monitored for survival over 72 h. Larvae were assessed at regular intervals and mortality was recorded when there were no signs of life after a gentle touch with forceps.

Data Analysis

All statistical analyses were performed using GraphPad Prism (GraphPad Software, San Diego, CA). For *M. sexta* survival assays, unpaired two-tailed Student's t-tests were used to compare the differences between experimental and control groups at defined time points.

CHAPTER THREE

RESULTS AND DISCUSSION

Generation of *C. glabrata STE11*$^{\Delta N346}$ truncation mutant

The *STE11* gene encodes a mitogen-activated protein kinase kinase kinase (MAPKKK), which plays a pivotal role in signal transduction pathways in fungi such as *S. cerevisiae* and *C. albicans*. For instance, in *S. cerevisiae*, the Ste11 protein transmits signals in response to environmental stimuli, such as pheromones and high osmolarity, eliciting responses related to mating, filamentous growth, and invasive behavior. Furthermore, in *C. albicans*, this MAPK cascade is crucial for maintaining cell wall construction and integrity (R. E. Chen & Thorner, 2007; T. Chen, Jackson, et al., 2019; Kim, Lee, & Choi, 1998; Ramezani Rad, Jansen, Bühring, & Hollenberg, 1998; Rhodes, Connell, & Errede, 1990; Stevenson, Rhodes, Errede, & Sprague, 1992) (See **Figure 1**).

The N-terminal region of this protein serves as a regulatory domain that detects upstream signals, initiating conformational modifications that activate it. As a result, removing this N-terminal region produces a truncated *STE11* mutant, *STE11*$^{\Delta N}$, which results in a constitutively active, or "hyperactive," form of the protein; this hyperactive mutant maintains continuous pathway activity and constantly stimulates downstream signaling components. For example, in *S. cerevisiae*, expression of a truncated Ste11 protein leads to continuous activation of the mating signaling pathway, even in the absence of external mating signals (Cairns, Ramer, & Kornberg, 1992). Also, in a clinically relevant context, a previous study examined the effects of β (1,3)-glucan exposure in *C. albicans* by generating a *STE11*$^{\Delta N467}$ mutant; the results showed that

hyperactivation of Ste11 leads to increased activation of the Cek1 MAPK pathway, which promotes cell wall unmasking. This unmasking enhances immune system recognition and has been linked to attenuated virulence (T. Chen, Jackson, et al., 2019). Therapeutically inducing constitutive activation of this signaling pathway represents a promising antifungal strategy, as persistent signaling can disrupt cellular homeostasis, impair cell wall integrity, and attenuate virulence in *C. albicans* and potentially other *Candida* species.

C. glabrata is a clinically significant pathogen associated with systemic candidiasis (Seider et al., 2014); however, it has been studied less extensively than *C. albicans*. Although effective treatment options are available, the emergence of antifungal resistance emphasizes the need for improved therapeutic approaches. Advancing our understanding of the biology of *C. glabrata*, including its mechanisms of infection and invasion, is critical for the development of more effective and targeted treatment strategies. Importantly, insights from *C. albicans* cannot be directly extrapolated to *C. glabrata* because of substantial biological and evolutionary differences between the two species. *Candida* species are classified into distinct phylogenetic clades: *C. albicans* belongs to the CTG clade, characterized by a codon switch from leucine to serine, whereas *C. glabrata* belongs to the whole-genome duplication (WGD) clade (Dujon et al., 2004). Phylogenetically, *C. glabrata* is more closely related to the budding yeast *S. cerevisiae* than to *C. albicans* (Dujon et al., 2004). Moreover, a study investigating *C. glabrata ste11* null mutants reported altered responses to hypertonic stress and attenuated virulence when compared to the wild-type strain (Calcagno et al., 2005).

This current study was guided by the hypothesis that hyperactivation of Ste11 in *C. glabrata* would lead to constitutive activation of MAPKs in the Ste11 cascades, resulting in increased β (1,3)-glucan exposure and attenuated virulence in a systemic model of infection. The central objective is based on the premise that targeting this signaling pathway represents a promising therapeutic strategy for combating infections caused by this organism. To assess the role of *STE11* in *C. glabrata*, a truncated form of the gene, $STE11^{\Delta N346}$, was constructed using the episomal plasmid pGRB2.1. This vector was selected for its reported improved transformation efficiency in *C. glabrata*, because of the presence of a species-specific CEN/ARS region. In contrast, the *S. cerevisiae* vector pRS316 was initially used as the vector, but due to failed experimental attempts a search of the literature reported that it functions less reliably in *C. glabrata* (Sikorski & Hieter, 1989; Zordan et al., 2013). The final construct, pGRB2.1-$STE11^{\Delta N346}$ was introduced into the wild-type *C. glabrata* strain Cg1 using the lithium acetate transformation method, following the protocol established for *S. cerevisiae* (Gietz & Schiestl, 2007). Transformants were selected on synthetic complete (SC) medium supplemented with complete supplement mixture without histidine and uracil (CSM-HIS-URA). PCR screening of four independent transformants confirmed the presence of the pGRB2.1-$STE11^{\Delta N346}$ construct (See **Figure 2**).

Effects of *C. glabrata* $STE11^{\Delta N346}$ truncation mutant on the MAPK pathway

A key regulatory system in eukaryotes is the mitogen-activated protein kinase (MAPK) pathway (Avruch, 2007). This highly conserved signaling module is characterized as a phosphorylation cascade involving three levels of kinases: a MAPK

kinase kinase (MAPKKK) phosphorylates and activates a MAPK kinase (MAPKK), which then phosphorylates and activates the final kinase, MAPK. This cascade begins when a ligand binds to and activates a cell-surface receptor, initiating a series of phosphorylation events that amplify the signal and alter gene expression within the nucleus (Cargnello & Roux, 2011). The *STE11$^{\Delta N467}$* truncation mutant in *C. albicans* was found to upregulate the Cek1 MAPK pathway, a mechanism responsible for repairing cell wall carbohydrate damage. This upregulation, in turn, led to the unmasking of β- (1,3) glucan and to attenuated virulence (T. Chen, Jackson, et al., 2019; van Wijlick, Swidergall, Brandt, & Ernst, 2016).

The effects of constitutive Ste11 activation in *C. glabrata* remain poorly understood, especially regarding MAPK pathway regulation. To begin addressing this gap, a western blot analysis was conducted to determine whether truncation of the Ste11 protein affects the MAPK signaling cascade similarly to what has been observed in *C. albicans*. Specifically, the experiment aimed to assess the phosphorylation status of MAPKs as an indicator of pathway activation. This approach was based on previous findings from Chen *et al.* (2019), who reported that disrupting phosphatidylserine (PS) synthase activity in a *C. albicans* cho1Δ/Δ mutant resulted in constitutive activation of the Cek1 and Mkc1 cascades. Additionally, a similar signaling pattern was observed in a gain-of-function *C. albicans* mutant expressing a truncated *STE11ΔN467* allele, where hyperactivation of Ste11 resulted in persistent activation of the Cek1 and Mkc1 pathways (T. Chen, Jackson, et al., 2019). These results provided the rationale for examining

whether analogous MAPK hyperactivation occurs in a *C. glabrata* Ste11 truncation mutant.

Detection of phosphorylated MAPKs in *C. glabrata* and *C. albicans* was achieved using the anti-phospho-p44/p42 MAPK antibody, as previously described (Jiménez-Sánchez, Cid, & Molina, 2007; Thomas et al., 2013). To investigate the effects of constitutively activating the *STE11* MAPK pathway, protein lysates were prepared from *C. glabrata* strains carrying the *STE11*$^{\Delta N346}$ mutation and wild-type controls, as well as from *C. albicans* strains with the *STE11*$^{\Delta N467}$ mutation and wild-type controls. The constitutive activation of phosphorylated MAPKs, Cek1 and Mkc1, was confirmed in the *C. albicans* and *STE11*$^{\Delta N467}$ mutant, as shown by western blot analysis (**Figure 3**) and consistent with previous findings. Phosphorylation levels of MAPKs in the *C. glabrata STE11ΔN346* mutant were comparable to those in the wild-type strain, the empty vector control, and the *C. albicans STE11*$^{\Delta N467}$ mutant. These results did not support the initial hypothesis that hyperactivation of Ste11 in *C. glabrata* would lead to constitutive activation of MAPKs in the Ste11 cascade. However, the *C. glabrata STE11*$^{\Delta N346}$ mutant showed no detectable changes in the MAPK phosphorylation of the predicted MAPKs Fus3, Kss1, and Slt2. These kinases were presumed based on their estimated molecular weights, with phosphorylated Fus3 appearing as a band at approximately 40 kDa, Kss1 at around 43 kDa, and Slt2 at about 56 kDa. Under the tested experimental conditions, truncation of *STE11* in *C. glabrata* did not significantly impact the MAPK signaling pathway, which remained active in both mutant and wild-type strains.

Unsuccessful introduction of *STE11$^{\Delta N467}$* into *C. albicans* clinical isolates

Previous studies in the *C. albicans* laboratory strain DAY286 (a derivative of SC5314) showed that continuous activation of the MAPK signaling pathway, achieved through the generation of a *STE11$^{\Delta N467}$* mutant, activated the Cek1 and Mkc1 cascades and resulted in increased β (1,3)-glucan exposure and attenuated virulence. (T. Chen, Jackson, et al., 2019). These findings prompted the question of whether a similar phenotype could be reproduced in clinical isolates of *C. albicans*. To investigate the role of *STE11$^{\Delta N467}$* in the clinical isolates p87, p75010, p57055, and p76067, a truncated allele was PCR-amplified from genomic DNA of the previously generated DAY286 *STE11$^{\Delta N467}$* mutant. However, despite multiple attempts at transformation, no colonies tested positive for the presence of the truncated *STE11$^{\Delta N467}$* allele. These results suggest that the linear DNA fragment was either not taken up, not integrated, or not stably maintained within the genome of these clinical isolates. Consequently, this strategy was considered ineffective for generating *STE11$^{\Delta N467}$* mutants in these clinical backgrounds. The observed transformation failure may be influenced by a variety of factors, including the inherent genomic plasticity of *C. albicans*. For instance, studies have repeatedly demonstrated that the *C. albicans* genome is susceptible to extensive chromosome reorganization, including translocations, truncations, and aneuploidy (Rustchenko, 2007; Selmecki, Forche, & Berman, 2010). These genomic variations are known to result in karyotypic differences among clinical isolates, which may account for transformation inefficiency, especially for protocols used in SC5314 (Rustchenko-Bulgac, 1991). Additionally, the decreased

transformation efficiency observed with linear DNA fragments is exacerbated by strain-specific differences (Corrigan, Kerwin-Iosue, Kuczmarski, Amin, & Wykoff, 2013).

Functional characterization of *CgCHO1* in *S. cerevisiae*

In the glycerophospholipid biosynthesis pathway for phosphatidylserine (PS), the enzyme PS synthase, Cho1p, catalyzes the reaction between cytidine diphosphate diacylglycerol (CDP-DAG) and serine to produce PS. PS can then be used directly by the cell or serve as a substrate for phosphatidylethanolamine (PE) biosynthesis, a reaction catalyzed by the PS decarboxylases Psd1p and Psd2p. (Y. L. Chen et al., 2010).

The metabolism of PS has been linked to the virulence of various microbial pathogens. For example, in the pathogen Brucella abortus, phosphatidylcholine (PC), a byproduct of PS synthesis, was shown to be crucial for virulence in a mouse model of infection. (Conde-Alvarez et al., 2006). In *Mycobacterium tuberculosis*, the loss of ino1, a gene necessary for phosphatidylinositol (PI) synthesis—derived from CDP-DAG biosynthesis—resulted in reduced virulence in SCID mice (Movahedzadeh et al., 2004). In the malaria parasite *Plasmodium falciparum*, inhibition of PE, a product of PS biosynthesis, led to cell growth defects and parasite death (Serrán-Aguilera et al., 2016). The phospholipids phosphatidylserine (PS) and phosphatidylethanolamine (PE) are associated with the virulence of *C. albicans* (Y. L. Chen et al., 2010; Rittershaus et al., 2006). However, the role of PS biosynthesis in *C. glabrata* remains poorly understood. Therefore, to investigate the function of PS in *C. glabrata* and its potential role in virulence, it was first necessary to characterize the function of the protein responsible for its production.

To examine the role of the CgCho1 protein, a trans-complementation method was employed by inserting the full-length CgCHO1 gene into the *S. cerevisiae* cho1Δ mutant, resulting in the strain Sccho1::CgCHO1. The *S. cerevisiae* cho1Δ mutant lacks endogenous PS synthase activity and shows a growth defect when ethanolamine is not supplemented. A PS synthase assay confirmed that *CgCHO1* restores PS synthase activity in the *S. cerevisiae* cho1Δ mutant. As shown in **Figure 4**, the Sccho1::CgCHO1 exhibited significantly elevated PS synthase activity compared to the cho1Δ mutant and empty vector control, even though the activity was slightly lower than the wild-type *S. cerevisiae*. These findings show that *CgCHO1* encodes a functional PS synthase enzyme capable of compensating for the loss of endogenous CHO1 in *S. cerevisiae*.

Spot dilution assays (see **Figure 5**) were conducted to further examine the ability of *CgCHO1* to complement the *S. cerevisiae* cho1Δ mutant functionally. As expected, the cho1Δ mutant failed to grow on minimal medium, but growth was restored when *CgCHO1* was expressed, indicating successful complementation. When supplemented with 1 mM of ethanolamine, the growth defect in the empty vector control was rescued, confirming the phenotype. Taken together, these results strongly indicate that *CgCHO1* encodes a functional PS synthase capable of compensating for the loss of enzymatic activity and the growth defect in *S. cerevisiae* cho1Δ mutant.

Virulence assessment in the *Manduca sexta* infection model

According to Lyons *et al.*, fifth instar *M. sexta* caterpillars are a suitable model for studying systemic fungal infections, including those caused by *C. albicans* (Lyons et al., 2020). To validate the usefulness of this model for investigating systemic candidiasis, we

examined the responses of caterpillars infected with *C. albicans* strains exhibiting varying levels of virulence, as previously observed in a murine model of systemic candidiasis. Overall, the observations and findings aligned with published data on different virulent *C. albicans* strains (T. Chen, Jackson, et al., 2019; Wagner et al., 2021) (**Figure 6**). The preliminary results showed that *M. sexta* caterpillars infected with the wild-type *C. albicans* strain had lower survival rates compared to those infected with the *C. albicans STE11*$^{\Delta N467}$ virulence-attenuated strain. (T. Chen, Jackson, et al., 2019; McLeish, 2021b; Wagner et al., 2021).

In addition to being used as an in vivo infection model for fungal pathogens, *M. sexta* larvae have also been utilized to study the *Steinernema-Xenorhabdus* entomopathogenic lifecycle. Within this lifecycle, *Xenorhabdus* bacteria are introduced into the insect host by *Steinernema* nematodes and eventually kill it. Consequently, to elucidate the mechanisms underlying the pathogenicity and toxicity associated with *Xenorhabdus* species, the survival profile of *M. sexta* was examined following infection with the bacteria. As described by Heppert *et al*., we assessed the entomopathogenic potential of several *Xenorhabdus* species, including *X. nematophila* (ATCC 19061), *X. innexi* (HGB1681), *X. griffiniae* (HGB2511 and ID10), and *Xenorhabdus* sp. TH1. Fifth instar *M. sexta* larvae were injected with approximately 1,000 bacterial cells in 10 μL of PBS, and survival was monitored over 72 hours. The survival analysis revealed strain-specific virulence profiles. For example, *X. nematophila* (ATCC 19061) caused the highest mortality, killing 90% of larvae, while *X. griffiniae* HGB2511 and *Xenorhabdus* sp. TH1 resulted in 60% and 70% mortality, respectively. (**Figure 7**). In contrast, *X.*

innexi HGB1681 and *X. griffiniae* ID10 were associated with lower virulence, exhibiting only 10% and 20% mortality, respectively (Heppert et al., 2024a). The results from these studies show that *M. sexta* larvae are vulnerable to both bacterial and fungal pathogens, confirming their utility as a versatile model for studying host-pathogen interactions, especially those that cross taxonomic kingdoms.

CHAPTER FOUR

CONCLUSIONS

This study used an integrative approach, combining molecular genetics, biochemical analysis, and *in vivo* infection models to examine the roles of specific genes and pathways in microbial pathogenesis. In order to characterize gene functions such as *STE11* and *CHO1*, evaluate virulence characteristics, and determine the usefulness of the non-mammalian host *Manduca sexta* for modelling systemic infections, the study focused on *Candida glabrata*, *Candida albicans,* and *Xenorhabdus* species. Using functional complementation assays, host-survival assessments, and gene-truncation and deletion mutants, this work provides insights into both conserved and diverse pathogenicity mechanisms in fungi and bacteria. The findings from this study enhance our broader understanding of infectious diseases and build upon previous research. For example, the *STE11*$^{\Delta N346}$ truncation mutation of *C. glabrata* was successfully expressed and validated, but unlike *C. albicans* (DAY286 *STE11*$^{\Delta N467}$ mutant), it did not show altered MAPK activation under the tested conditions. This differs from earlier findings in *C. albicans* and suggests the possibility of a compensatory mechanism or regulatory pathway divergence in *C. glabrata*. These species-specific variations among *Candida* highlight the need for more comparative functional analyses to evaluate potential antifungal targets.

Additionally, this work confirmed *CgCHO1* as a phosphatidylserine (PS) synthase through functional complementation in a *S. cerevisiae* cho1Δ mutant. Since phospholipid metabolism is essential for fungal survival, membrane stability, and stress responses, CgCHO1 is a promising target for further research in developing antifungal drugs (Zhou

et al., 2024). Its functional conservation further supports its usefulness in examining gene functions across different fungi species.

Furthermore, using *M. sexta* as a model host for fungal and bacterial pathogens showed the usefulness and reliability of invertebrate systems in infection research. This model accurately recapitulated known virulence traits of *C. albicans* DAY286 *STE11*$^{\Delta N467}$ mutants and uncovered differences in virulence among *Xenorhabdus* species (T. Chen, Jackson, et al., 2019; T. Chen, Wagner, et al., 2019; Heppert et al., 2024b). These results confirm that *M. sexta* is a robust and ethically acceptable alternative to vertebrate models for evaluating host immune responses and pathogenicity. Moreover, expanding the scope of this model to include entomopathogenic bacteria alongside fungi enhances its suitability for studying host-pathogen interactions.

Taken together, these findings highlight the importance of combining cellular and molecular methods to study complex microbial mechanisms and demonstrate how model systems like M. sexta can serve as practical tools for both basic and translational infectious disease research. Future directions

Although this research provides significant insight into the molecular and pathogenic mechanisms of *Candida* and *Xenorhabdus*, several areas may require further study. Future research, building on the present findings, could investigate the following queries:

1. <u>*C. glabrata* MAPK Pathways: A Mechanistic Analysis.</u> The unexpected MAPK activation in the *C. glabrata* wild-type and *STE11*$^{\Delta N346}$ truncation mutant raises essential questions about the structure and regulation of this signaling cascade.

Future research could use transcriptomic profiling to discover downstream targets or compensatory signaling pathways. A more realistic comparison with *S. cerevisiae*, due to its close phylogenetic relationship, might be more helpful in understanding the cascades rather than comparing it to *C. albicans*, as was initially guided to do. Additionally, epistasis experiments with other MAPK pathway components, such as HOG1 and CEK1 orthologs, may clarify STE11's role in stress adaptation and virulence.

2. Clinical Isolates of *C. albicans*: Genetic Tools. The difficulty in genetically manipulating *C. albicans* clinical isolates (p87, p75010, p57055, and p76067) underscores the need for optimized transformation protocols or alternative genome-editing strategies, such as CRISPR-Cas9 systems and the split-marker approach. The development of stable integrative vectors or inducible expression systems tailored to clinical strain backgrounds would significantly improve functional genomics across various *Candida* species.
3. Further analysis of phospholipid biosynthesis and lipidomic in *C. glabrata*. Although it has been demonstrated that *CgCHO1* encodes a functional phosphatidylserine (PS) synthase, additional research is needed to fully understand lipid metabolism in *C. glabrata*. It may be beneficial to perform lipidomic profiling of *CgCHO1* deletion mutants, particularly under stress conditions, to reveal compensatory pathways or potential lethality. Additionally, perform a comparative cell wall analysis of the *C. glabrata* WT, cho1Δ, and cho1Δ::CHO1 strains using immunofluorescence staining, flow cytometry, and

transmission electron microscopy. The data generated from this may elucidate the function of the PS synthase enzyme in the cell wall organization of *C. glabrata*. Furthermore, the virulence of the Cgcho1Δ mutant can be evaluated using *M. sexta* fifth instar caterpillars by measuring survival after infection and determining fungal burden in the insect's hemolymph and feces through colony-forming unit (CFU) plating assays.

Technical and conceptual skills gained

During the course of the research, a broad range of technical skills and an understanding of fundamental concepts in infection biology and molecular microbiology were developed. The experimental study required expertise in molecular cloning techniques, which are crucial for functional genomics and include plasmid design, restriction-ligation, Gibson assembly, colony screening, and PCR optimization. Developed expertise in microbial transformation techniques using both chemical and electroporation methods for various species, including *E. coli, S. cerevisiae*, *C. glabrata*, and *C albicans*.

Western blotting was also mastered for protein expression analysis, including lysate preparation, SDS-PAGE, antibody probing, and phospho-specific antibody analysis of kinase activity. Assessing the functional effects of STE11 truncation on MAPK signaling required these abilities.

A key component of the research was the *in vivo* experimental design, specifically the development and application of the *M. sexta* infection model. Accurate injection dosage preparation, animal observation, and survival analysis using statistical tools were

all necessary for this research to be successful. Designing and interpreting virulence assays in a non-mammalian system broadened understanding of host-pathogen interactions and showed how different models are relevant for translation.

The efforts of this thesis deepened my understanding of the complexities of the host immune response, the genes of pathogenic fungi, and the conservation of metabolic pathways across species. It also strengthened my critical thinking, hypothesis development, and experimental troubleshooting skills, which are essential for success in academic and translational research settings.

LIST OF REFERENCES

Avruch, J. (2007). MAP kinase pathways: the first twenty years. *Biochimica et Biophysica Acta (BBA)-Molecular Cell Research, 1773*(8), 1150-1160.

Beardsley, J., Kim, H. Y., Dao, A., Kidd, S., Alastruey-Izquierdo, A., Sorrell, T. C., . . . Bongomin, F. (2024). Candida glabrata (Nakaseomyces glabrata): A systematic review of clinical and microbiological data from 2011 to 2021 to inform the World Health Organization Fungal Priority Pathogens List. *Medical Mycology, 62*(6), myae041.

Bertero, A., Brown, S., & Vallier, L. (2017). Methods of cloning. In *Basic science methods for clinical researchers* (pp. 19-39): Elsevier.

Bhattacharya, S., Sae-Tia, S., & Fries, B. C. (2020). Candidiasis and mechanisms of antifungal resistance. *Antibiotics, 9*(6), 312.

Bradford, M. M. (1976). A rapid and sensitive method for the quantitation of microgram quantities of protein utilizing the principle of protein-dye binding. *Analytical biochemistry, 72*(1-2), 248-254.

Brown, G. D., Denning, D. W., Gow, N. A., Levitz, S. M., Netea, M. G., & White, T. C. (2012). Hidden killers: human fungal infections. *Science translational medicine, 4*(165), 165rv113-165rv113.

Brunke, S., & Hube, B. (2013). Two unlike cousins: C andida albicans and C. glabrata infection strategies. *Cellular microbiology, 15*(5), 701-708.

Cairns, B., Ramer, S., & Kornberg, R. (1992). Order of action of components in the yeast pheromone response pathway revealed with a dominant allele of the STE11

kinase and the multiple phosphorylation of the STE7 kinase. *Genes & development, 6*(7), 1305-1318.

Calcagno, A.-M., Bignell, E., Rogers, T. R., Jones, M. D., Mühlschlegel, F. A., & Haynes, K. (2005). Candida glabrata Ste11 is involved in adaptation to hypertonic stress, maintenance of wild-type levels of filamentation and plays a role in virulence. *Medical Mycology, 43*(4), 355-364.

Cargnello, M., & Roux, P. P. (2011). Activation and function of the MAPKs and their substrates, the MAPK-activated protein kinases. *Microbiology and molecular biology reviews, 75*(1), 50-83.

Chen, R. E., & Thorner, J. (2007). Function and regulation in MAPK signaling pathways: lessons learned from the yeast Saccharomyces cerevisiae. *Biochimica et Biophysica Acta (BBA)-Molecular Cell Research, 1773*(8), 1311-1340.

Chen, T., Jackson, J. W., Tams, R. N., Davis, S. E., Sparer, T. E., & Reynolds, T. B. (2019). Exposure of Candida albicans β (1, 3)-glucan is promoted by activation of the Cek1 pathway. *PLoS genetics, 15*(1), e1007892.

Chen, T., Wagner, A. S., Tams, R. N., Eyer, J. E., Kauffman, S. J., Gann, E. R., . . . Reynolds, T. B. (2019). Lrg1 regulates β (1, 3)-glucan masking in Candida albicans through the Cek1 MAP kinase pathway. *MBio, 10*(5), e01767-01719.

Chen, Y. L., Montedonico, A. E., Kauffman, S., Dunlap, J. R., Menn, F. M., & Reynolds, T. B. (2010). Phosphatidylserine synthase and phosphatidylserine decarboxylase are essential for cell wall integrity and virulence in Candida albicans. *Molecular microbiology, 75*(5), 1112-1132.

Conde-Alvarez, R., Grilló, M. J., Salcedo, S. P., De Miguel, M. J., Fugier, E., Gorvel, J. P., . . . Iriarte, M. (2006). Synthesis of phosphatidylcholine, a typical eukaryotic phospholipid, is necessary for full virulence of the intracellular bacterial parasite Brucella abortus. *Cellular microbiology, 8*(8), 1322-1335.

Corrigan, M. W., Kerwin-Iosue, C. L., Kuczmarski, A. S., Amin, K. B., & Wykoff, D. D. (2013). The fate of linear DNA in Saccharomyces cerevisiae and Candida glabrata: the role of homologous and non-homologous end joining. *PloS one, 8*(7), e69628.

Cottier, F., & Hall, R. A. (2020). Face/off: The interchangeable side of Candida albicans. *Frontiers in Cellular and Infection Microbiology, 9*, 471.

De Backer, M. D., Maes, D., Vandoninck, S., Logghe, M., Contreras, R., & Luyten, W. H. (1999). Transformation of Candida albicans by electroporation. *Yeast, 15*(15), 1609-1618.

Dujon, B., Sherman, D., Fischer, G., Durrens, P., Casaregola, S., Lafontaine, I., . . . Talla, E. (2004). Genome evolution in yeasts. *Nature, 430*(6995), 35-44.

Eleftherianos, I., Clarke, D. J., Dowling, A. J., & Reynolds, S. E. (2010). Dissecting the immune response to the entomopathogen Photorhabdus. *Trends in microbiology, 18*(12), 552-560.

Garcia-Bustos, V., Pemán, J., Ruiz-Gaitán, A., Cabañero-Navalon, M. D., Cabanilles-Boronat, A., Fernández-Calduch, M., . . . Tormo-Mas, M. Á. (2022). Host–pathogen interactions upon Candida auris infection: fungal behaviour and immune response in Galleria mellonella. *Emerging microbes & infections, 11*(1), 136-146.

Gardner, M. B., & Luciw, P. A. (2008). Macaque models of human infectious disease. *ILAR journal, 49*(2), 220-255.

Giammarino, A., Bellucci, N., & Angiolella, L. (2024). Galleria mellonella as a Model for the Study of Fungal Pathogens: Advantages and Disadvantages. *Pathogens, 13*(3), 233.

Gietz, R. D., & Schiestl, R. H. (2007). High-efficiency yeast transformation using the LiAc/SS carrier DNA/PEG method. *Nature protocols, 2*(1), 31-34.

Goodrich-Blair, H., & Clarke, D. J. (2007). Mutualism and pathogenesis in Xenorhabdus and Photorhabdus: two roads to the same destination. *Molecular microbiology, 64*(2), 260-268.

Green, M. R., & Sambrook, J. (2012). Molecular cloning. *A Laboratory Manual 4th, 448*.

Healey, K. R., & Perlin, D. S. (2018). Fungal resistance to echinocandins and the MDR phenomenon in Candida glabrata. *Journal of Fungi, 4*(3), 105.

Heppert, J. K., Awori, R. M., Cao, M., Chen, G., McLeish, J., & Goodrich-Blair, H. (2024a). Analyses of Xenorhabdus griffiniae genomes reveal two distinct sub-species that display intra-species variation due to prophages. *BMC genomics, 25*(1), 1087.

Heppert, J. K., Awori, R. M., Cao, M., Chen, G., McLeish, J., & Goodrich-Blair, H. (2024b). Analyses of Xenorhabdus griffiniae genomes reveal two distinct sub-species that display intra-species variation due to prophages. *bioRxiv*, 2024.2003. 2008.584182.

Hetzler, L., Kollef, M. H., Yuenger, V., Micek, S. T., & Betthauser, K. D. (2022). New antimicrobial treatment options for severe Gram-negative infections. *Current Opinion in Critical Care, 28*(5), 522-533.

Hickson, S. M., Ledger, E. L., & Wells, T. J. (2025). Emerging antimicrobial therapies for Gram-negative infections in human clinical use. *npj Antimicrobials and Resistance, 3*(1), 16.

Huang, M. Y., Woolford, C. A., May, G., Mcmanus, C. J., & Mitchell, A. P. (2019). Circuit diversification in a biofilm regulatory network. *PLoS pathogens, 15*(5), e1007787.

Hussa, E., & Goodrich-Blair, H. (2012). Rearing and injection of Manduca sexta larvae to assess bacterial virulence. *JoVE (Journal of Visualized Experiments)*(70), e4295.

Ikuta, K. S., Swetschinski, L. R., Aguilar, G. R., Sharara, F., Mestrovic, T., Gray, A. P., . . . Hayoon, A. G. (2022). Global mortality associated with 33 bacterial pathogens in 2019: a systematic analysis for the Global Burden of Disease Study 2019. *The Lancet, 400*(10369), 2221-2248.

Jiménez-Sánchez, M., Cid, V. J., & Molina, M. (2007). Retrophosphorylation of Mkk1 and Mkk2 MAPKKs by the Slt2 MAPK in the yeast cell integrity pathway. *Journal of Biological Chemistry, 282*(43), 31174-31185.

Kaiser, C., Michaelis, S., & Mitchell, A. (1994). *Methods in yeast genetics* (Vol. 234): Cold Spring Harbor Laboratory Press Cold Spring Harbor, NY.

Kim, S.-H., Lee, S.-K., & Choi, K.-Y. (1998). Saccharomyces cerevisiae STE11 may contribute to the stabilities of a scaffold protein, STE5, in the pheromone signaling pathway. *Molecules and cells, 8*(2), 130-137.

Kondaka, K., Sappati, S., Rząd, K., Paluszkiewicz, E., Maciejewska, N., Baginski, M., & Gabriel, I. (2025). Bisacridine derivatives as effective eukaryotic topoisomerase II inhibitors. *European Journal of Medicinal Chemistry*, 118174.

Lionakis, M. S., & Netea, M. G. (2013). Candida and host determinants of susceptibility to invasive candidiasis. *PLoS pathogens, 9*(1), e1003079.

Lyons, N., Softley, I., Balfour, A., Williamson, C., O'Brien, H. E., Shetty, A. C., . . . Diezmann, S. (2020). Tobacco Hornworm (Manduca sexta) caterpillars as a novel host model for the study of fungal virulence and drug efficacy. *Virulence, 11*(1), 1075-1089.

Mayer, F., Wilson, D., & Hube, B. (2013). Candida albicans pathogenicity mechanisms. Virulence 4: 119–128. In.

McLeish, J. (2021a). Unpublished data.

McLeish, J. (2021b). Unpulished.

McQuade, R., & Stock, S. P. (2018). Secretion systems and secreted proteins in Gram-negative entomopathogenic bacteria: their roles in insect virulence and beyond. *Insects, 9*(2), 68.

Movahedzadeh, F., Smith, D. A., Norman, R. A., Dinadayala, P., Murray-Rust, J., Russell, D. G., . . . Bancroft, G. J. (2004). The Mycobacterium tuberculosis ino1 gene is essential for growth and virulence. *Molecular microbiology, 51*(4), 1003-1014.

Nakayama, H., Izuta, M., Nagahashi, S., Sihta, E. Y., Sato, Y., Yamazaki, T., . . . Kitada, K. (1998). A controllable gene-expression system for the pathogenic fungus Candida glabrata. *Microbiology, 144*(9), 2407-2415.

Oh, D. Y., & Hurt, A. C. (2016). Using the ferret as an animal model for investigating influenza antiviral effectiveness. *Frontiers in microbiology, 7*, 80.

Pappas, P. G., Lionakis, M. S., Arendrup, M. C., Ostrosky-Zeichner, L., & Kullberg, B. J. (2018). Invasive candidiasis. *Nature reviews Disease primers, 4*(1), 1-20.

Pfaller, M. A., Diekema, D. J., Turnidge, J. D., Castanheira, M., & Jones, R. N. (2019). *Twenty years of the SENTRY antifungal surveillance program: results for Candida species from 1997–2016.* Paper presented at the Open forum infectious diseases.

Ramezani Rad, M., Jansen, G., Bühring, F., & Hollenberg, C. (1998). Ste50p is involved in regulating filamentous growth in the yeast Saccharomyces cerevisiae and associates with Ste11p. *Molecular and General Genetics MGG, 259*(1), 29-38.

Rhodes, N., Connell, L., & Errede, B. (1990). STE11 is a protein kinase required for cell-type-specific transcription and signal transduction in yeast. *Genes & development, 4*(11), 1862-1874.

Richard, M. L., Nobile, C. J., Bruno, V. M., & Mitchell, A. P. (2005). Candida albicans biofilm-defective mutants. *Eukaryotic cell, 4*(8), 1493-1502.

Ricotta, E. E., Lai, Y. L., Babiker, A., Strich, J. R., Kadri, S. S., Lionakis, M. S., . . . Adjemian, J. (2021). Invasive candidiasis species distribution and trends, United States, 2009–2017. *The Journal of Infectious Diseases, 223*(7), 1295-1302.

Rittershaus, P. C., Kechichian, T. B., Allegood, J. C., Merrill, A. H., Hennig, M., Luberto, C., & Del Poeta, M. (2006). Glucosylceramide synthase is an essential regulator of pathogenicity of Cryptococcus neoformans. *The Journal of clinical investigation, 116*(6), 1651-1659.

Rustchenko, E. (2007). Chromosome instability in Candida albicans. *FEMS yeast research, 7*(1), 2-11.

Rustchenko-Bulgac, E. P. (1991). Variations of Candida albicans electrophoretic karyotypes. *Journal of bacteriology, 173*(20), 6586-6596.

Sarkar, S., & Heise, M. T. (2019). Mouse models as resources for studying infectious diseases. *Clinical therapeutics, 41*(10), 1912-1922.

Seider, K., Gerwien, F., Kasper, L., Allert, S., Brunke, S., Jablonowski, N., . . . Kuchler, K. (2014). Immune evasion, stress resistance, and efficient nutrient acquisition are crucial for intracellular survival of Candida glabrata within macrophages. *Eukaryotic cell, 13*(1), 170-183.

Selmecki, A., Bergmann, S., & Berman, J. (2005). Comparative genome hybridization reveals widespread aneuploidy in Candida albicans laboratory strains. *Molecular microbiology, 55*(5), 1553-1565.

Selmecki, A., Forche, A., & Berman, J. (2010). Genomic plasticity of the human fungal pathogen Candida albicans. *Eukaryotic cell, 9*(7), 991-1008.

Serrán-Aguilera, L., Denton, H., Rubio-Ruiz, B., López-Gutiérrez, B., Entrena, A., Izquierdo, L., . . . Hurtado-Guerrero, R. (2016). Plasmodium falciparum choline

kinase inhibition leads to a major decrease in phosphatidylethanolamine causing parasite death. *Scientific reports, 6*(1), 1-12.

Sikorski, R. S., & Hieter, P. (1989). A system of shuttle vectors and yeast host strains designed for efficient manipulation of DNA in Saccharomyces cerevisiae. *Genetics, 122*(1), 19-27.

Stevenson, B. J., Rhodes, N., Errede, B., & Sprague, G. (1992). Constitutive mutants of the protein kinase STE11 activate the yeast pheromone response pathway in the absence of the G protein. *Genes & development, 6*(7), 1293-1304.

Thomas, E., Roman, E., Claypool, S., Manzoor, N., Pla, J., & Panwar, S. L. (2013). Mitochondria influence CDR1 efflux pump activity, Hog1-mediated oxidative stress pathway, iron homeostasis, and ergosterol levels in Candida albicans. *Antimicrobial agents and chemotherapy, 57*(11), 5580-5599.

Trevijano-Contador, N., & Zaragoza, O. (2014). Expanding the use of alternative models to investigate novel aspects of immunity to microbial pathogens. *Virulence, 5*(4), 454-456.

Tsai, C. J.-Y., Loh, J. M. S., & Proft, T. (2016). Galleria mellonella infection models for the study of bacterial diseases and for antimicrobial drug testing. *Virulence, 7*(3), 214-229.

van Wijlick, L., Swidergall, M., Brandt, P., & Ernst, J. F. (2016). Candida albicans responds to glycostructure damage by Ace2-mediated feedback regulation of Cek1 signaling. *Molecular microbiology, 102*(5), 827-849.

Wagner, A. S., Hancock, T. J., Lumsdaine, S. W., Kauffman, S. J., Mangrum, M. M., Phillips, E. K., . . . Reynolds, T. B. (2021). Activation of Cph1 causes ß (1, 3)-glucan unmasking in Candida albicans and attenuates virulence in mice in a neutrophil-dependent manner. *PLoS pathogens, 17*(8), e1009839.

Xiong, L., Goerlich, K., Do, E., & Mitchell, A. P. (2024). Strain variation in the Candida albicans iron limitation response. *Msphere, 9*(7), e00372-00324.

Zhao, Y., Wang, C.-L., Gao, Z.-Y., Qiao, H.-X., Wang, W.-J., Liu, X.-Y., & Chuai, X. (2023). Ferrets: A powerful model of SARS-CoV-2. *Zoological Research, 44*(2), 323.

Zhou, Y., Phelps, G. A., Mangrum, M. M., McLeish, J., Phillips, E. K., Lou, J., . . . Lee, R. E. (2024). The small molecule CBR-5884 inhibits the Candida albicans phosphatidylserine synthase. *MBio*, e00633-00624.

Zordan, R. E., Ren, Y., Pan, S.-J., Rotondo, G., Peñas, A. D. L., Iluore, J., & Cormack, B. P. (2013). Expression plasmids for use in Candida glabrata. *G3: Genes, Genomes, Genetics, 3*(10), 1675-1686.

APPENDIX

FIGURES

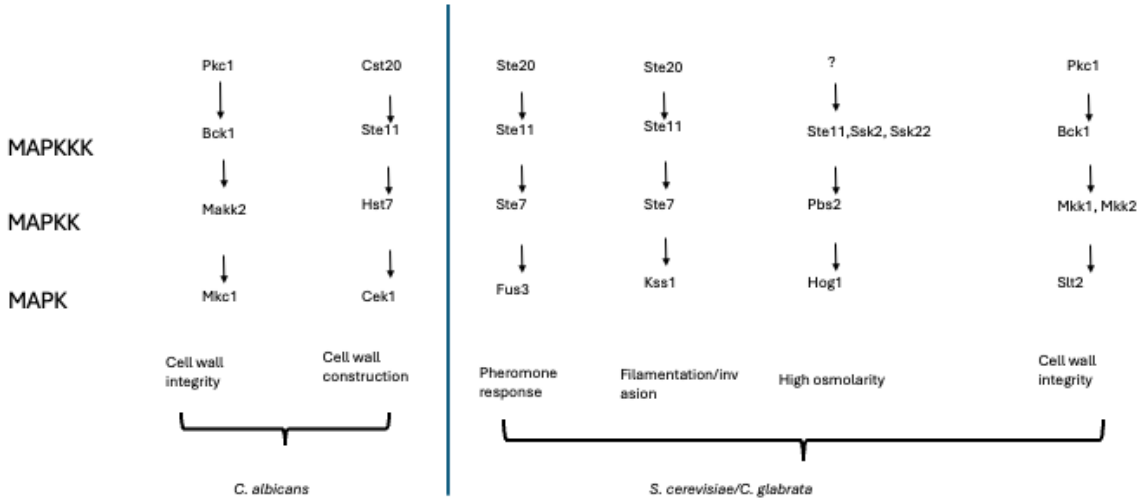

Figure 1. MAPK modules in *C. albicans, C. glabrata* and *S. cerevisiae*. The two branches on the left of the illustration represent *C. albicans* MAPK pathways that have been implicated in the cho1Δ/Δ and *STE11*$^{\Delta N467}$ mutants which leads to increased β (1,3) glucan exposure and attenuated virulence; the MAPKKK Ste11 phosphorylates the MAPKK Hst7 which in turn phosphorylates the MAPK Cek1. The four branches on the right of the illustration represent the MAPK pathways in *S. cerevisiae* and *C. glabrata*; the MAPKKK Ste11 phosphorylates the MAPKK Ste7 or Pbs2 which in turn phosphorylates Fus3, Kss1 and Hog1.

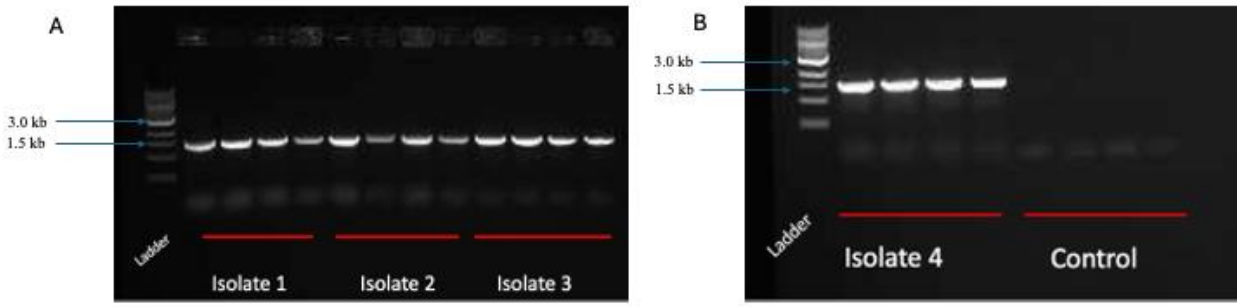

Figure 2. PCR verification of pGRB2.1-STE11$^{\Delta N346}$ construct in *C. glabrata* transformants. (A) Cg1STE11$^{\Delta N346}$ isolates 1, 2, and 3 (B) Cg1STE11$^{\Delta N346}$ isolate 4 and an untransformed Cg1 wild-type control. A 1-kb DNA ladder was included for size estimation. The presence of the ~1500 bp band confirms the successful transformation of pGRB2.1-STE11$^{\Delta N346}$ into Cg1.

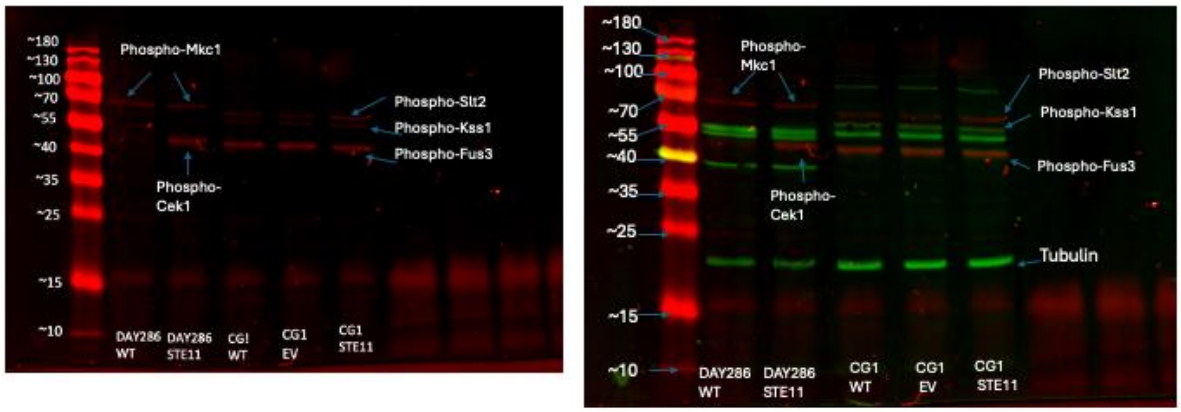

Figure 3. Western blot analysis of phosphorylated MAPKs in *C. glabrata* and *C. albicans*. Whole cell lysates were prepared from wild-type and *STE11$^{\Delta N}$* mutant strains of *C. glabrata* and *C. albicans,* and phosphorylated MAPKs were detected using an anti-phospho-p44/p42 antibody (red bands), an ERK-type MAPK antibody. No detectable differences in phosphorylated MAPKs were observed in the *C. glabrata STE11$^{\Delta N346}$* and wild-type strains. In contrast, differences were observed in the *C. albicans* strains, as was previously reported; the DAY286 *STE11$^{\Delta N467}$* strain showed phosphorylated Cek1, whereas the wild-type did not. However, in both strains of *C. albicans*, Mkc1 phosphorylation was observed. The green bands represent rat tubulin, used as a loading control.

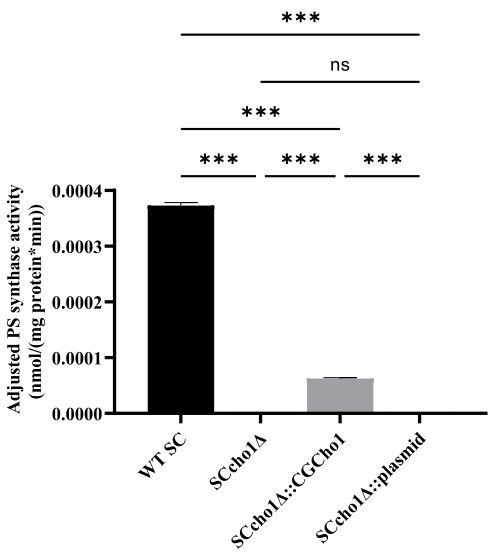

Figure 4. Phosphatidylserine synthase activity in *S. cerevisiae* expressing *CgCHO1*. Adjusted PS synthase activity was observed in *S. cerevisiae* wild-type (WT SC), *S. cerevisiae* cho1Δ (SC cho1Δ), *S. cerevisiae* cho1Δ::CgCHO1 (Sccho1Δ::CGcho1), and *S. cerevisiae* cho1Δ + empty vector (Sccho1Δ::plasmid). Sccho1Δ::CGcho1 exhibited significantly elevated PS synthase activity compared to Sccho1Δ and empty vector controls, and slightly lower activity compared to wild-type *S. cerevisiae*. ***p < 0.001. n.s. = not significant.

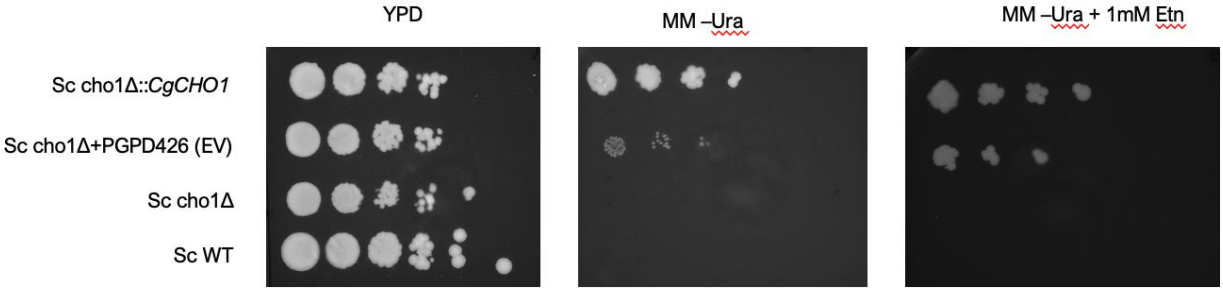

Figure 5. *CgCHO1* complements the growth defect in the *S. cerevisiae* cho1Δ mutant. *S. cerevisiae* wild-type (Sc WT), *S. cerevisiae* cho1Δ (Sc cho1Δ), *S. cerevisiae* + empty vector (Sc cho1Δ + pGDP426), and *S. cerevisiae* cho1Δ expressing *CgCHO1* (Sc cho1Δ::CgCHO1) were grown in YPD, minimal medium lacking uracil (MM -Ura) and minimal medium lacking uracil and supplemented with 1 mM ethanolamine (MM -Ura +1mM Etn). 5 µL of cells were spotted onto plates in serial dilutions (1:10), and after three days of incubation at 30 °C growth was measured. The expression of *CgCHO1* in the *S. cerevisiae* cho1Δ mutant restored the lost growth defect.

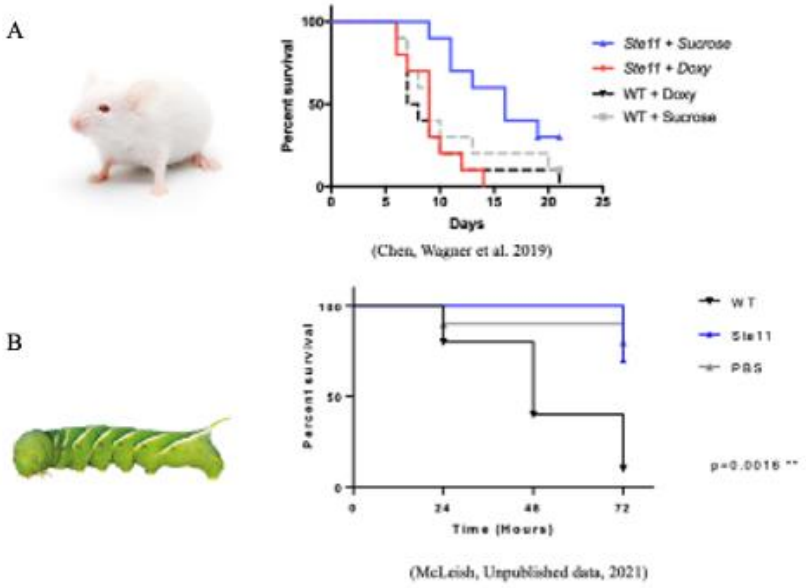

Figure 6. Hyperactive STE11$^{\Delta N467}$ leads to attenuated virulence in animal models of systemic infection. (A) Survival curve of mice infected with C. albicans strains expressing hyperactive STE11$^{\Delta N467}$ and wild-type, under doxycycline- or sucrose-inducible conditions. Mice infected with the STE11$^{\Delta N467}$ strain exhibited significantly higher survival compared to those infected with wild-type strains, particularly under doxycycline-induced conditions, indicating reduced virulence (T. Chen, Wagner, et al., 2019). (B) M. sexta caterpillar survival following infection with C. albicans STE11$^{\Delta N467}$ or wild-type strains in the same conditions. Infection with STE11$^{\Delta N467}$ resulted in significantly higher caterpillar survival compared to wild-type, which was consistent with observations in the murine model ($p = 0.0016$). PBS-injected larvae served as negative controls (McLeish, 2021a).

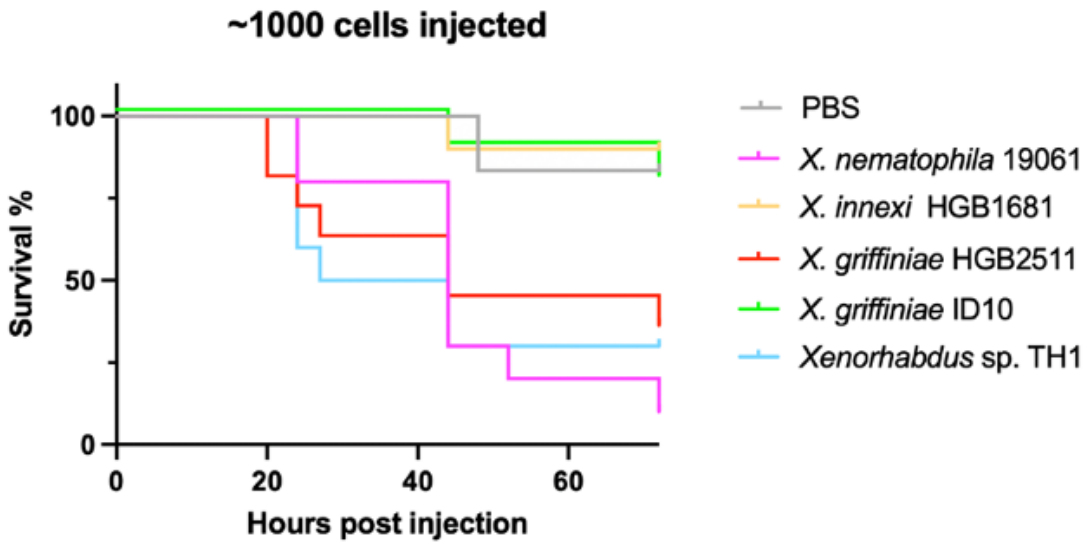

Figure 7. Comparative entomopathogenicity of *Xenorhabdus* species in *M. sexta* larvae. Survival curves of fifth instar larvae infected with ~1,000 cells of *X. nematophila* 19061, *X. innexi* HGB1681, *X. griffiniae* HGB2511 and ID10, or *Xenorhabdus* sp. TH1. PBS injection served as a negative control. Survival was monitored for up to 72 hours.

TABLES

Table 5.1. Strains used in this study.

Strain	Species	Description	Reference/Source
DH5α	*E. coli*		Thermo Fisher Scientific
Cg1	*C. glabrata*	wild-type strain	Lab collection
CgSTE11$^{\Delta N346}$	*C. glabrata*	*STE11* truncated mutant	This study
DAY286	*C. albicans*	wild-type clinical strain	Lab collection
DAY286 STE11$^{\Delta N467}$	*C. albicans*	*STE11* truncated mutant	Lab collection
p87	*C. albicans*	wild-type clinical strain	Lab collection
p75010	*C. albicans*	wild-type clinical strain	Lab collection
p57055	*C. albicans*	wild-type clinical strain	Lab collection
p76067	*C. albicans*	wild-type clinical strain	Lab collection
SC5314	*S. cerevisiae*	wild-type strain	Lab collection
SC5314 cho1Δ	*S. cerevisiae*	*CHO1* deletion mutant	Lab collection

Table 5.2. Plasmids used in this study.

Plasmid	Characteristic	Source/Reference
pRS316	YC-type (CEN/ARS) shuttle vector	Lab collection
pGRB2.1 (p157)	URA3 TRP1 ARS1, Amp^r Tet^r CEN/ARS episomal	Lab collection
pRS306		Lab collection
pCgCho1Δ	Knock out plasmid made in pRS306 backbone	This study
pAG25	Vector with NAT1 resistant cassette	Lab collection
pWTF-STE11$^{\Delta 467}$	Split-marker knockout vector for *C. albicans* clinical strains	Lab collection
pGPD426 (p426 GPD)	Overexpression vector for CgCHO1 expression in *S. cerevisiae*	Lab collection
pCgCho1Δ with NAT1 cassette	Knockout construct with integrated NAT1 cassette	This study
pINTG4	tetR::GAL4AD integrating	(Nakayama et al., 1998)
p97CGH	*CgHIS3*, *tetO*::*ScHOP1*-gene	(Nakayama et al., 1998)
p99CGH	*CgHIS3*, *tetO*::*ScHOP1*-gene	(Nakayama et al., 1998)

Table 5.3. Oligonucleotides used in this study.

Primer	Sequence (5'-3')	Restriction site	Purpose
AWO156	GGTAATATCATCGATGAACAG	N/A	*STE11* Forward Primer (at -512, roughly 500bp downstream of the homologous region for the *STE11Δ*^{N467} doxy insert (that's at -1))
AWO157	CAACATCGATTGAACTGAAC	N/A	*STE11* Reverse Primer (at +1906, roughly 500bp downstream of the homologous region for the *STE11*$^{\Delta N467}$ doxy insert (that's at +1401))
JMO7	AAAAAAGCTTGCTCTGACGAGAGTGAAGAAGAAA	*Hind*III	Forward for 5'NCR of CgCHO1 used in making pcgcho1Δ

Table 2.3. Continued

Primer	Sequence (5'-3')	Restriction site	Purpose
JMO8	AAAAGAATTCCTATTTCTCGTCACTGCAACAA	*EcoR*I	Reverser for 5'NCR of CgCHO1 used in making pcgcho1 Δ
JMO9	AAAAGAATTCTCCACCCCATAATTACCTGTCT	*EcoR*I	Forward for 3'NCR of CgCHO1 used in making pcgcho1 Δ
JMO10	AAAAGGATCCTTTGGTGTGGTTCGTAGTGTAGA	*BamH*I	Reverse for 3'NCR of CgCHO1 used in making pcgcho1 Δ

Table 2.3. Continued

Primer	Sequence (5'-3')	Restriction site	Purpose
JMO11	AAAAAAGCTTGTGACTGTAAAAGTAGGCGTAGTG	*Hind*III	Forward for 5' NCR of CgSLT2
JMO12	AAAAGAATTCGATTTGTAGGATACGCTAGAATTTC	*EcoR*I	Reverse for 5' NCR of CgSLT2
JMO13	AAAAGAATTCTTCACATGCAGTTACAGAGCAAA	*EcoR*I	Forward for 3' NCR of CgSLT2
JMO14	AAAAGGATCCTTGGCAATGGATTGCATCTC	*BamH*I	Reverse 3' NCR of CgSLT2

Table 2.3. Continued

Primer	Sequence (5'-3')	Restriction site	Purpose
JMO15	AAAAGAATTCCAGCTGAAGCTTCGTACGC	*EcoRI*	Forward for NAT1 Cassette (from pAG25)
JMO16	AAAAGAATTCGCATAGGCCACTAGTGGATCTG	*EcoRI*	Reverse for NAT1 Cassette (from pAG25)
JMO17	AAAAGGTACCGCTCTGACGAGAGTGAAGAAGAAA	*KpnI*	Forward for 5'NCR of CgCHO1 used for amplifying CgCHO1 to put into pGRB2.1
JMO18	AAAAGGATCC AGGAGAGGTAAGCCAGCTTTT	*BamHI*	Forward primer (5'CgCHO1) for *S. cerevisiae cho1Δ* mutant in pGPD426
JMO19	AAAAAAGCTTTCATGGCTTAGGGATCTTCA	*HindIII*	Reverse primer (3'CgCHO1) for *S. cerevisiae cho1Δ* mutant in pGPD426

Table 2.3. Continued

Primer	Sequence (5'-3')	Restriction site	Purpose
JMO20	ATCACATCTACCTTGAGC	Null	Reverse for Hygromycin B marker in pWTF-STE11 sequence
JMO21	GATGCAATTGTCTGAAG	Null	Forward for Hygromycin B marker in pWTF-STE11 sequence
JMO22	GTTGCAGTGACGAGAAATAGGcagctgaagcttcgtacg	Null	Forward for NgCho1-NAT1-k/o
JMO23	CAGGTAATTATGGGGTGGAGgcataggccactagtgg	Null	Reverse for NgCho1-NAT1-k/o
JMO24	AGTTCTGTAGGTCCTGGCAAT 5'ATTGCCAGGACCTACAGAACT 3'	Null	Reverse primer for NgCho1-NAT1-k/o in ~700 bp 3'UTR of CHO1 (to verify correct position of 5'UTR-NAT1cassette-3'UTR fragment)

VITA

Jemma McLeish attended Andrews University for her undergraduate and graduate studies before attending graduate school at the University of Tennessee-Knoxville during the 2020 SARS-CoV-2 pandemic. She is very grateful for the support and experience she received at UT and is hugely excited to continue her career.